Pergamon

Int. J. Heat Mass Transfer. Vol. 40, No. 2, pp. 281–293, 1997

0017–9310/97 $15.00 + 0.00

PII: S0017–9310(96)00113–5

Numerical investigation of adsorptive heat pump systems with thermal wave heat regeneration under uniform-pressure conditions

L. M. SUN, Y. FENG† and M. PONS
LIMSI–CNRS, B.P. 133, 91403 Orsay, France

(*Received* 4 *April* 1995 *and in final form* 20 *March* 1996)

Abstract—A numerical analysis of an adsorptive heat pump system with thermal wave heat regeneration is presented, using a two-dimensional model taking into account axial heat transfer in the circulating fluid and radial heat conduction in the adsorbent bed. The axial heat conduction in the adsorbent bed is neglected, allowing the two-dimensional model to be solved as a one-dimensional one. The time constants for heat exchange and heat conduction in the adsorbent bed are derived using the moment analysis and can be used to quantify the relative importance of the two heat transfer processes. The effects of the thermal conductivity and the cycle time on the process performance are also presented. Copyright © 1996 Elsevier Science Ltd.

1. INTRODUCTION

In recent years, adsorption has attracted increasing attention in the refrigeration and air-conditioning industries in the concern to replace the traditional compressor-based refrigeration using ozone harmful CFCs and HCFCs. The adsorptive refrigeration and heat pumps make use of benign fluids, such as water, ammonia and alcohols, and constitute one of the most promising alternatives [1–4].

In the basic adsorptive heat pump systems, the adsorbers play the role of the compressors by alternatively adsorbing an adsorbate coming from an evaporator and desorbing the adsorbate into a condenser. These systems have virtually no moving parts and are therefore very simple and reliable. However, the performance of such systems is too low to be economically competitive and a considerable performance enhancement is necessary. Recent studies have shown that the improvement of the performance of adsorptive heat pumps can be achieved by making significant progresses in the following directions [5]: (1) development of new adsorbate-adsorbent systems which have good properties for the working pressure and the shape of adsorption isotherms; (2) development of new adsorbers with intensified heat and mass transfer properties; and finally (3) design of more efficient cyclic processes.

Recently, a regenerative cycle using the thermal wave principle has been proposed to improve the performance of adsorptive systems [6, 7]. With this cycle, two adsorbent beds operate 180° out of phase and a fluid circulates between the two beds in order to recover the heat energy. The heat regeneration could be very efficient if the temperature fronts established in the fluid are very sharp [8, 9]. The sharpness of temperature fronts depends mostly on the rates of heat transfer processes which are perpendicular to the flow direction and on the ratio of heat capacities of the circulating fluid and the adsorber. The radial heat transfer processes include heat exchange between the circulating fluid and a metal tube, heat exchange between the tube and the adsorber, and the heat conduction inside the adsorber. The faster the rates of these heat transfer processes, the sharper the temperature fronts. It has been reported that the cooling coefficient of performance (*COP*) of such regenerative systems can exceed 1, which is considerably higher than the *COP* of basic adsorption cycles [10].

The efficiency of the thermal wave regenerative system depends on a relatively large number of parameters: for example, rates of various heat transfer processes, the flow rate of the circulating fluid, the cycle time, the adsorber configuration, etc. It is clear that an optimal design of these systems would require detailed modelling and numerical simulations based on physically realistic and numerically cost-effective models. In most of the thermal adsorption devices, the adsorber is heated/cooled indirectly by an external heat transfer fluid. With this configuration, the major limitation comes from the heat transfer resistances perpendicular to the flow direction of the heat transfer fluid including the resistances at the interface and inside the adsorbent bed, as a result of relatively poor

† Present address: Department of Chemical Engineering, South China University of Technology, Guang Zhou, People's Republic of China.

NOMENCLATURE

a	$=R_0/R_1$
c	specific heat [J kg^{-1} K^{-1}]
COP	cooling coefficient of performance
C_S	volumetric heat capacity of the adsorbent defined in equation (11) [J m^{-3} K^{-1}]
D_f	thermal dispersion coefficient [m^2 s^{-1}]
h	heat transfer coefficient, unit surface conductance [W m^{-2} K^{-1}]
h_{eff}	global unit surface conductance defined in equations (30) and (32) [W m^{-2} K^{-1}]
ΔH	heat of adsorption [J kg^{-1}]
K_P	derivative with respect to pressure [kg m^{-3} Pa^{-1}]
K_T	derivative with respect to temperature [kg m^{-3} K^{-1}]
L	length of the adsorber [m]
L_v	latent heat of vaporization [J kg^{-1}]
Δm	mass of adsorbate evaporated from the evaporator [kg]
M_{ads}	mass of the adsorbent [kg]
N_r	number of computational grids in the radial direction
N_z	number of computational grids in the axial direction
P	gas phase pressure [Pa]
PCP	mean power of cold production per unit of adsorbent mass [W (kg adsorbent)$^{-1}$]
P_s	saturated vapor pressure [Pa]
q	adsorbed phase concentration [kg m^{-3}]
Q_h	heat input of the heater [J]
r	radial coordinate in the adsorbent bed [m]
R_0	inner radius of the adsorbent bed [m]
R_1	outer radius of the adsorbent bed [m]
R_2	external radius of the adsorber [m]
S	heat transfer surface area [m^2]
t	time [s]
t_c	cycle time [s]
t_h	time constant for the heat exchange between the bed and the tube [s]
t_λ	time constant for the heat conduction in the adsorbent bed [s]
T	temperature [K]
v	flow velocity [m s^{-1}]
V	volume [m^3]
z	spatial coordinate in the axial direction [m].

Greek symbols

λ	thermal conductivity [W m^{-1} K^{-1}]
ρ	density [kg m^{-3}].

Subscripts

0	initial state
a	adsorbed phase
c	cooling
co	condenser
ev	evaporator
f	fluid, interface fluid–tube
h	heating
i	grid index in the radial direction
j	grid index in the axial direction
m	tube
s	adsorbent bed, interface tube–adsorbent.

Superscripts

n	time level.

heat transfer properties of usual adsorbent beds. This limitation results generally in the use of relatively long cycle times to ensure acceptable performances. With long cycles, the effect of the limitation by mass transfer inside the adsorber could be negligible and use of a pure heat transfer model which assumes that the gas pressure is uniform throughout the adsorbent bed could be realistic. The validity of this assumption could be further justified in the case of high working pressure adsorbates like ammonia as a result of low flow resistances in the adsorbent bed.

In this paper, we will present a numerical analysis of the thermal wave regenerative adsorption cycle using a pure heat transfer model. This model is basically two-dimensional as heat transfer occurs both in the (axial) flow direction and in the radial direction. However, it will be shown that such a model can be numerically solved as a one-dimensional model if the axial heat conduction in the adsorbent bed can be neglected. This simplifying condition could be reasonable provided that the rate of axial heat conduction in the adsorber is much slower than that of thermal propagation of the heat transfer fluid. This is usually the case in practical applications. A direct consequence of neglecting the axial heat conduction in the adsorber is that the resulting numerical model requires much less computation time and therefore is well adapted for the process design and optimization.

2. DESCRIPTION OF A REGENERATIVE CYCLE

In a thermal wave regenerative adsorption cycle, six major components are used: two adsorbent beds, a fluid heater, a fluid cooler, a condenser and an evaporator (Fig. 1). Initially, bed 1 is assumed to be cool and is to be heated while the other bed is hot and is

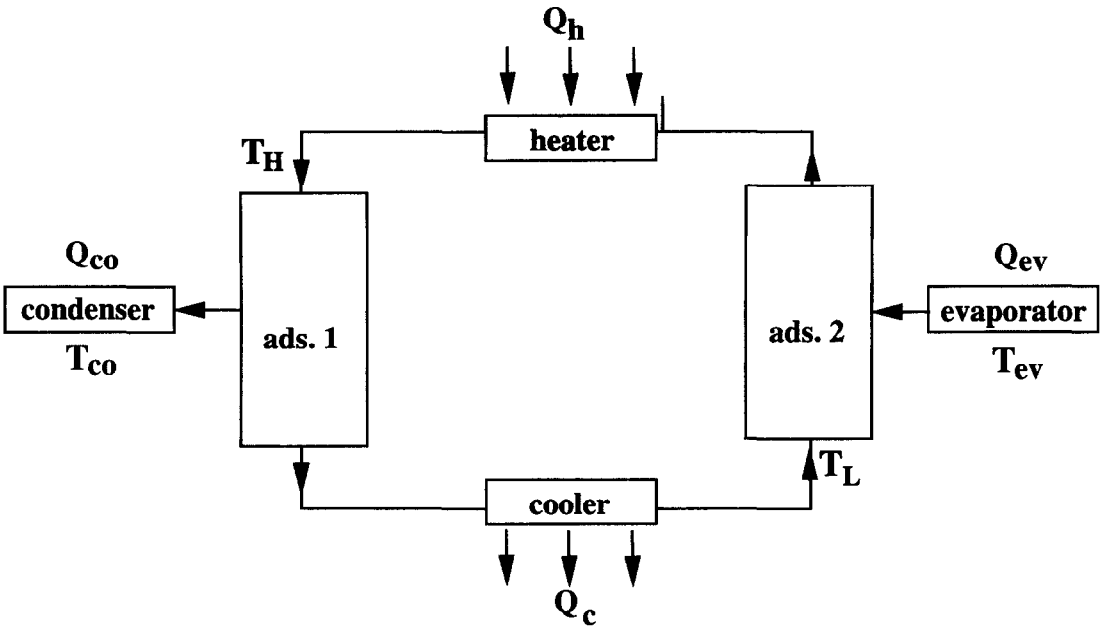

Fig. 1. Principle of a thermal wave regenerative adsorption heat pump system.

to be cooled. A heat transfer fluid circulates between the two beds via a reversible pump. After coming out of the heater, the fluid has a high temperature T_H. Then, it passes into the cool bed, heating the bed and at the same time being cooled. The fluid goes then into the fluid cooler and is further cooled to a low temperature T_L. After the cooler, the cool fluid passes in the hot bed 2 for the cooling and finally gets back to the heater. The fluid circulation continues until the bed 1 is sufficiently heated and bed 2 is sufficiently cooled.

During the heating of bed 1, it is firstly closed (that is, isosteric heating) and therefore the gas pressure inside the bed increases. Once the pressure becomes larger than the pressure in the condenser, the bed is opened to the condenser and the desorbed adsorbate is condensed in the condenser. Similarly, the cooling of bed 2 is firstly made in an isosteric way until the gas pressure in the bed decreases down to the pressure in the evaporator. After this, bed 2 is connected to the evaporator and the fluid in the evaporator will evaporate and be re-adsorbed in bed 2.

This is the first half of the regenerative cycle. The second half cycle consists of circulating the fluid in the reverse direction. During this second half cycle, bed 1 is cooled while bed 2 is heated. The cooling COP and the mean power of cold production per unit of adsorbent mass for the present regenerative system are defined as:

$$COP = \frac{Q_{ev}}{Q_h} = \frac{\Delta m L_v}{Q_h} \tag{1}$$

$$PCP = \frac{Q_{ev}}{M_{ads} t_c} \tag{2}$$

where Δm is the mass of adsorbate evaporated into the adsorbers during a cycle, L_v is the latent heat of vaporization, Q_h is the heat input of the fluid heater, M_{ads} is the mass of the adsorbent and t_c is the time of a complete cycle. Herein, the energy used by the reversible pump is assumed to be negligible.

With the present configuration, it is only necessary to analyze one bed as the other bed operates under exactly the same cyclic conditions, but one half-cycle out of phase.

3. MATHEMATICAL MODEL

The central element for a regenerative adsorptive heat pump is an adsorbent bed which is heated or cooled by a circulating fluid through a metal tube (Fig. 2). The adsorber is of cylindrical shape and the circulating heat transfer fluid can be located either inside or outside the adsorbent bed. The major assumptions used for the model development are:

- The mass transfer inside the adsorbent bed is infinitely fast so that the pressure is always kept uniform in the adsorber. This means that the amount adsorbed in the adsorbent can be simply related to the gas pressure and the adsorbent temperature through an adsorption equilibrium equation.
- The local thermal equilibrium is satisfied, that is, the adsorbent and the adsorbate have the same temperature.
- Heat conduction in the axial direction is neglected both in the tube and in the adsorbent bed. This means that the rates of axial heat conduction in the tube and in the adsorber are assumed to be very slow compared to that of thermal wave propagation of the heat transfer fluid.
- Most of the model parameters, such as the flow

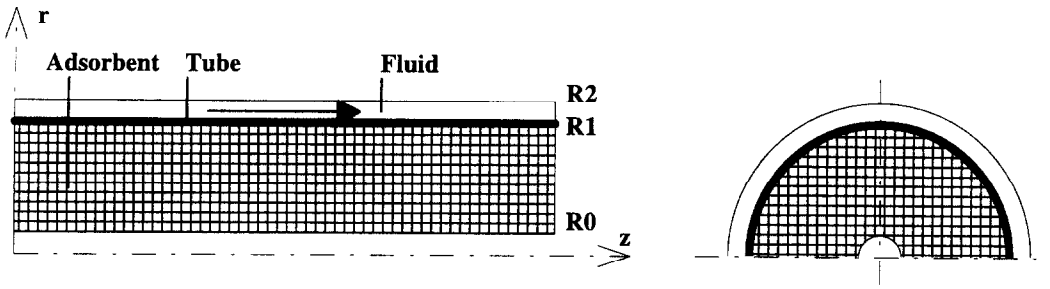

Fig. 2. Schematic representation of the adsorber.

velocity, densities, heat transfer coefficients and the heat of adsorption, are considered to be constant. The adsorption equilibrium relation is, however, nonlinear.

- No heat losses are considered.

The energy equation for the circulating fluid is:

$$\frac{\partial T_f}{\partial t}+v\frac{\partial T_f}{\partial z}-D_f\frac{\partial^2 T_f}{\partial z^2}+\frac{h_f S_f}{V_f\rho_f c_f}(T_f-T_m)=0 \quad (3)$$

where T_f and T_m are temperatures of the fluid and tube, respectively. v is the flow velocity. V_f, ρ_f and c_f are, respectively, volume, density and specific heat of the fluid. h_f and S_f are heat transfer coefficient and surface area at the interface fluid–tube. The coefficient D_f represents thermal dispersion in the fluid caused both by axial heat conduction and by velocity gradients which are perpendicular to the flow direction. In the case of the laminar flow in a tube, this coefficient can be determined by analogy to the mass dispersion using the Taylor–Aris theory [11]:

$$D_f=\frac{\lambda_f}{\rho_f c_f}+\frac{4R^2v^2\rho_f c_f}{192\lambda_f} \quad (4)$$

where λ_f is the thermal conductivity of the fluid, R is the tube radius and v is the mean velocity.

The boundary conditions for the fluid temperature are given by:

during the heating:

$$T_f|_{z=0}=T_H \quad (5)$$

$$\left.\frac{\partial T_f}{\partial z}\right|_{z=L}=0 \quad (6)$$

during the cooling:

$$\left.\frac{\partial T_f}{\partial z}\right|_{z=0}=0 \quad (7)$$

$$T_f|_{z=L}=T_L \quad (8)$$

where L is the length of the adsorber.

The energy equation for the tube is given by:

$$V_m\rho_m c_m\frac{\partial T_m}{\partial t}+h_f S_f(T_m-T_f)+h_s S_s(T_m-T_s|_{t-s})=0 \quad (9)$$

where V_m, ρ_m and c_m are volume, density and specific heat of the metal tube, respectively. h_s and S_s are the unit surface conductance and surface area at the interface tube–adsorber. $T_s|_{t-s}$ is the adsorbent temperature at the interface tube–adsorber, that is, at $r=R_0$ for the internal heating/cooling, or at $r=R_1$ for the external heating/cooling.

The heat balance in the adsorbent bed is given by the Fourier equation:

$$C_S\frac{\partial T_s}{\partial t}-|\Delta H|\frac{\partial q}{\partial t}=\frac{\lambda_s}{r}\frac{\partial}{\partial r}\left(r\frac{\partial T_s}{\partial r}\right) \quad (10)$$

where C_S is the volumetric heat capacity of the adsorbent bed including the solid and the adsorbed phase; $|\Delta H|$ is the heat of adsorption; q is the amount adsorbed in the adsorbent; and λ_s is the apparent thermal conductivity of the adsorbent bed. Neglecting the heat capacity of the gas phase, the volumetric heat capacity of the adsorbent is given by:

$$C_S=\rho_s c_s+qc_a \quad (11)$$

where ρ_s and c_s are the density and specific heat of the adsorbent, and c_a is the specific heat of the adsorbed phase. In this work, we assume that c_a is equal to the specific heat of the liquid phase. The adsorbed amount, q, can be related to the gas pressure P and the adsorbent temperature T_s using an adsorption equilibrium equation:

$$\frac{\partial q}{\partial t}=\left(\frac{\partial q}{\partial P}\right)_{T_s}\frac{dP}{dt}+\left(\frac{\partial q}{\partial T_s}\right)_P\frac{\partial T_s}{\partial t}=K_P\frac{dP}{dt}-K_T\frac{\partial T_s}{\partial t} \quad (12)$$

where the derivative parameters K_P and K_T are in general nonlinear functions of P and T_s. The heat conduction equation (10) can be rewritten as:

$$(C_S+|\Delta H|K_T)\frac{\partial T_s}{\partial t}-K_P|\Delta H|\frac{dP}{dt}-\frac{\lambda_s}{r}\frac{\partial}{\partial r}\left(r\frac{\partial T_s}{\partial r}\right)=0. \quad (13)$$

The boundary conditions for the above heat conduction equation are:

internal heating/cooling:

$$-\lambda_s \left.\frac{\partial T_s}{\partial r}\right|_{r=R_0} = h_s(T_m - T_s|_{r=R_0}) \tag{14}$$

$$\left.\frac{\partial T_s}{\partial r}\right|_{r=R_1} = 0 \tag{15}$$

external heating/cooling:

$$\left.\frac{\partial T_s}{\partial r}\right|_{r=R_0} = 0 \tag{16}$$

$$-\lambda_s \left.\frac{\partial T_s}{\partial r}\right|_{r=R_1} = h_s(T_s|_{r=R_1} - T_m). \tag{17}$$

By integrating the heat conduction equation (13) over the adsorber section $[R_0, R_1]$, we obtain:

$$\frac{2}{R_1^2 - R_0^2}\int_{R_0}^{R_1}\left[(C_S + |\Delta H|K_T)\frac{\partial T_s}{\partial t} - K_P|\Delta H|\frac{dP}{dt}\right] r\,dr = \frac{h_s S_s}{V_s}(T_m - T_s|_{r=s}). \tag{18}$$

Using the above equation, the tube equation (9) can be rearranged as:

$$\frac{\partial T_m}{\partial t} + \frac{\alpha_s}{\alpha_m} I_m + H_f(T_m - T_f) = 0 \tag{19}$$

with

$$\alpha_m = \frac{V_m \rho_m c_m}{V_f \rho_f c_f}; \quad \alpha_s = \frac{V_s C_e}{V_f \rho_f c_f}; \quad H_f = \frac{h_f S_f}{V_m \rho_m c_m}$$

$$I_m = \frac{2}{C_e(R_1^2 - R_0^2)}\int_{R_0}^{R_1}\left[(C_S + |\Delta H|K_T)\frac{\partial T_s}{\partial t} - K_P|\Delta H|\frac{dP}{dt}\right] r\,dr$$

where the total volume of the adsorber $V_s = \pi(R_1^2 - R_0^2)\,L$ and C_e represents the quantity $C_S + |\Delta H|K_T$ calculated at an arbitrarily-chosen reference state (at the initial state for example).

Elimination of the exchange term $h_f S_f(T_f - T_m)$ from the fluid equation (3) yields the following overall heat balance equation:

$$\frac{\partial T_f}{\partial t} + v\frac{\partial T_f}{\partial z} - D_f\frac{\partial^2 T_f}{\partial z^2} + \alpha_m\frac{\partial T_m}{\partial t} + \alpha_s I_m = 0. \tag{20}$$

The gas pressure in the adsorber, P, is maintained constant when the adsorber is opened to the condenser/evaporator, and is determined from the constant-volume condition when the adsorber is closed. In the latter case, the mass of adsorbate contained in the adsorber remains constant and the variation of the gas pressure is calculated from the following integral equation:

$$\frac{d}{dt}\left(\int_0^L\int_{R_0}^{R_1} qr\,dr\,dz\right) = 0. \tag{21}$$

For the initial condition, a uniform distribution for the temperatures is assumed here:

$$T_f(z) = T_m(z) = T_s(r,z) = T_0 \quad \text{and} \quad P = P_0. \tag{22}$$

Finally, it is noted that in the limiting case of infinitely-fast radial heat conduction, the heat balance for the adsorber can simply reduce to:

$$V_s C_S\frac{\partial T_s}{\partial t} - V_s|\Delta H|\frac{\partial q}{\partial t} = h_s S_s(T_m - T_s). \tag{23}$$

4. METHOD OF SOLUTION

The above set of equations contains four unknowns: the fluid temperature T_f, the tube temperature T_m, the adsorbent temperature T_s and finally the gas pressure P. T_f and T_m are functions of the time and only the axial position while T_s depends on both the axial and radial positions. The gas pressure is only a function of the time and is to be determined from the integral equation (21). We can note that heat transfers in the axial and radial directions are only coupled through boundary conditions as a result of neglecting the axial heat conduction in the tube and adsorber. Therefore, the present two-dimensional problem can be considered as one-dimensional (in the axial direction) with source terms depending on heat transfer in the radial direction.

This set of equations is solved numerically using an implicit finite difference method with the second-order Crank–Nicolson scheme. The spatial discretization in the axial direction is done with a constant step (Δz). For the spatial discretization in the radial direction, an equal spacing is used when the circulating fluid is inside. When the fluid is outside, an iso-volumetric discretization is applied. This iso-volumetric discretization proved to be considerably more efficient than the equal-spacing discretization [12].

The heat conduction equation (13) for the adsorbent bed is first discretized using the central differencing scheme, leading to a tridiagonal system. The Thomas's algorithm is then applied, but without performing completely the back solution procedure since the boundary conditions contain the tube temperature which is still unknown. However, it is relatively easy to extract a linear relation between the adsorbent temperature and the tube temperature (see Appendix B for the details):

$$T_{si,j}^{n+1} = F_{i,j} + G_{i,j}T_{mj}^{n+1} \tag{24}$$

where n is the index for the time level, i and j are, respectively grid indexes in the radial and axial direc-

tions, $F_{i,j}$ and $G_{i,j}$ are coefficients determined from Thomas's algorithm. This method is similar to that proposed by von Rosenberg for the treatment of non-linear boundary conditions [13]. Introducing the above equation into the discretized tube equation (19), we can obtain:

$$T_{mj}^{n+1} = A_j + B_j T_{fj}^{n+1}. \tag{25}$$

Thus, the source terms appearing in the fluid equation (10) can be replaced by linear expressions of the fluid temperature T_f. The convection term in this equation is approximated using the quadratic upstream differencing scheme (QUDS) proposed by Leonard [14]. The QUDS offers a significant improvement over the first-order upstream differencing and second-order differencing schemes and is well adapted for adsorption dynamics simulations [15]. The diffusion term is replaced by its second-order central differencing analog. This results in a quadridiagonal system for the fluid temperature which can be readily solved using a Thomas-type algorithm. Once the fluid temperature, T_f, is known, a back solution procedure is performed to calculate T_m and T_s using equations (24) and (25).

Solution of the gas pressure

For the calculation of the gas pressure during the constant-volume process, an iterative procedure is applied. Starting with an old value of the pressure, P^n, one calculates new temperatures using the solution procedure discussed above. These new temperature values are introduced in the integral equation (21), leading to a nonlinear equation for P^{n+1}. This nonlinear equation is then solved iteratively using the Newton–Raphson method or the Brent method [16]. The calculation continues until the difference in the temperature values obtained between two iterations is small enough. In the present work, a value of 10^{-5} is used for the relative errors. Note that this iterative process includes the necessary adjustment of the non-constant coefficients that are due to the adsorption equilibrium (K_P and K_T) and that make the equations nonlinear. Compared to a direct global solving (i.e. introduction of the pressure among the unknowns to be solved implicitly) this procedure has several advantages: (i) it is much faster. Indeed, the present method involves only solution of quadridiagonal matrice with a computational cost only linearly proportional to the total number of unknowns N. However, when the global solution method is used, solution of full matrices is required as the temperature of the fluid, tube and adsorbent at all the grids are coupled, the computational cost becomes much higher ($\sim N^3$ if the Gauss elimination method is used). (ii) The present numerical scheme is as well-adapted to the constant volume (isosteric) process as to the constant pressure process. As a consequence, the whole cycle is modelled with only one numerical scheme. Finally, (iii) solution of problems with different boundary conditions (for instance, prescribed adsorbed (desorbed) vapour flow-rate, condenser or evaporator with varying temperature, etc.) can be easily included.

5. DEFINITION OF THE GLOBAL HEAT TRANSFER CONDUCTANCE FOR THE ADSORBENT BED

Two different radial heat transfer resistances are simultaneously involved in the overall transfer rate of the adsorbent bed: the heat transfer resistances at the external surface with the tube, characterized by the unit surface conductance, h_s, and the heat conduction inside the bed characterized by the apparent thermal conductivity, λ_s. From a practical point of view, it is often useful to define a global heat transfer conductance which accounts for both effects. As the process studied herein is of dynamic nature, it would be erroneous to use the definitions derived from the stationary heat conduction solution. In this work, we will apply the moment method to determine the global surface conductance. The moment method is largely used in the chromatographic analysis [17] and in the adsorption kinetics study [18].

Consider the following linear heat conduction equation:

$$C_e \frac{\partial T_s}{\partial t} = \frac{\lambda_s}{r} \frac{\partial}{\partial r}\left(r \frac{\partial T_s}{\partial r}\right). \tag{26}$$

The boundary conditions are given by an adiabatic condition at the inner side and a heat exchange at the outer side:

$$\left.\frac{\partial T_s}{\partial r}\right|_{r=R_0} = 0 \tag{27}$$

$$-\lambda_s \left.\frac{\partial T_s}{\partial r}\right|_{r=R_1} = h_s(T_s|_{r=R_1} - T_1) \tag{28}$$

where T_1 is the constant temperature of the surroundings which is different from the initial temperature T_0.

Solving the above equations in the Laplace domain and using van der Laan's theorem [17], we can obtain the zero-order moment of the volumetrically averaged temperature:

$$\int_0^\infty \left(1 - \frac{\bar{T}_s - T_0}{T_1 - T_0}\right) dt = \frac{1-a^2}{2}\frac{R_1 C_e}{h_s} + \left[\frac{1+a^2}{8} - \frac{a^2}{2}\left(\frac{a^2 \ln a}{1-a^2} + 1\right)\right]\frac{R_1^2 C_e}{\lambda_s} = t_h + t_\lambda \tag{29}$$

where $a = R_0/R_1$ and $\bar{T}_s$ represents the volumetric average value of T_s. It can be noted that this zero-order moment is equal to the sum of two time constants: t_h for the heat exchange and t_λ for the heat conduction.

Table 1. Parameter values used in the numerical simulations

$R_0 = 2$ mm	$R_1 = 10$ mm	$R_2 = 13$ mm
$L = 1$ m	$v = 0.01$ m s^{-1}	$D_f = 10^{-5}$ m^2 s^{-1}
$\Delta H = -1.5 \times 10^6$ J kg^{-1}	$\rho_s = 640$ kg m^{-3}	$c_s = 840$ J kg^{-1} K^{-1}
$c_a = 3000$ J kg^{-1} K^{-1}	$h_f = 1000$ W m^{-2} K^{-1}	$h_s = 1000$ W m^{-2} K^{-1}
$\alpha_m = 0.065$	$\alpha_s = 0.789$	$T_H = 260$°C
$T_L = 20$°C	$T_{co} = 40$°C	$T_{ev} = 5$°C
$L_v(T_{ev}) = 1.24 \times 10^6$ J kg^{-1}	$P_0 = 5.12$ bar	$T_0 = 20$°C

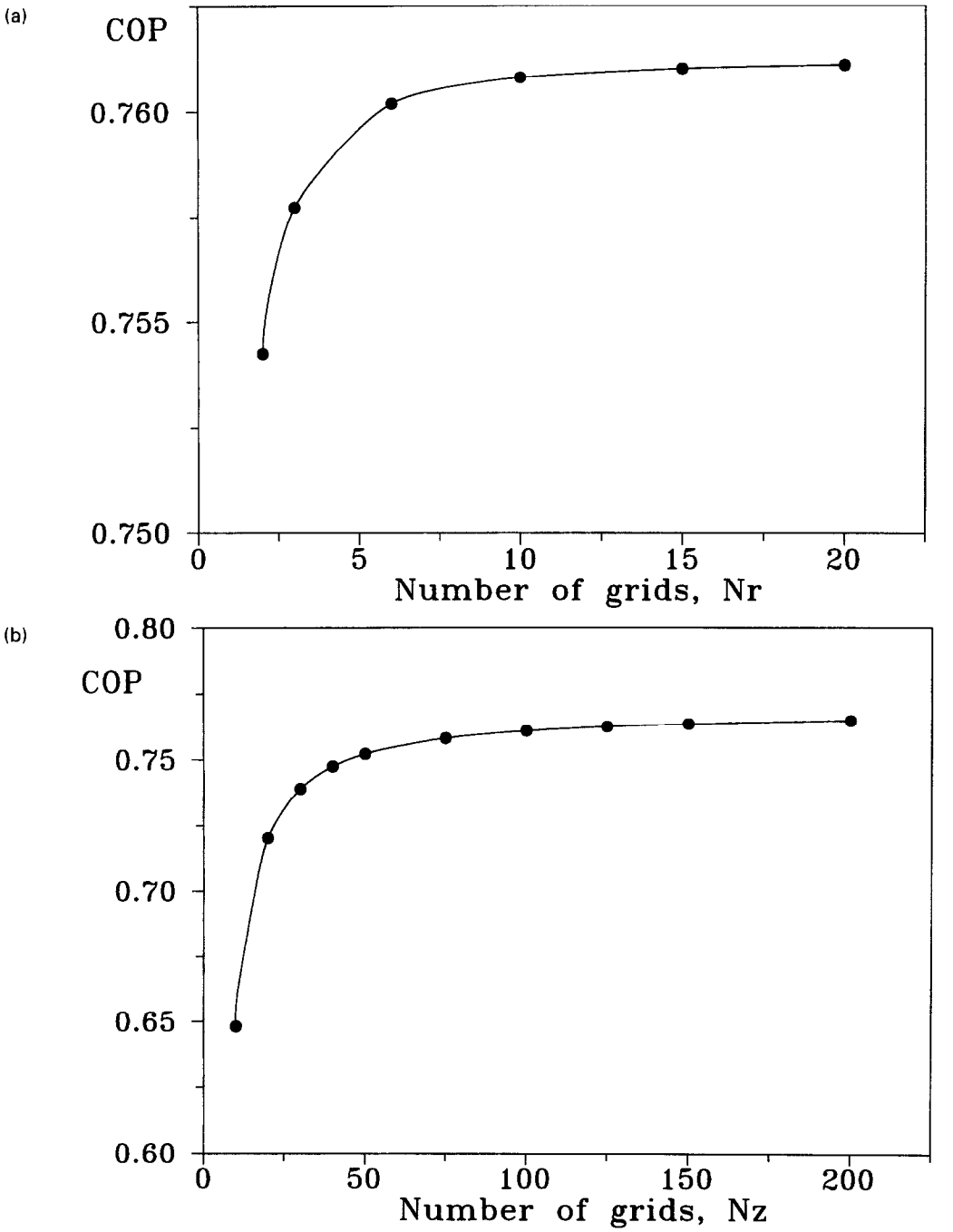

Fig. 3. Cooling *COP*s obtained at the cyclically steady state for different numbers of computational grids in the axial direction (a, with $N_r = 10$) and in the radial direction (b, with $N_z = 100$). The cycle time is 240 s.

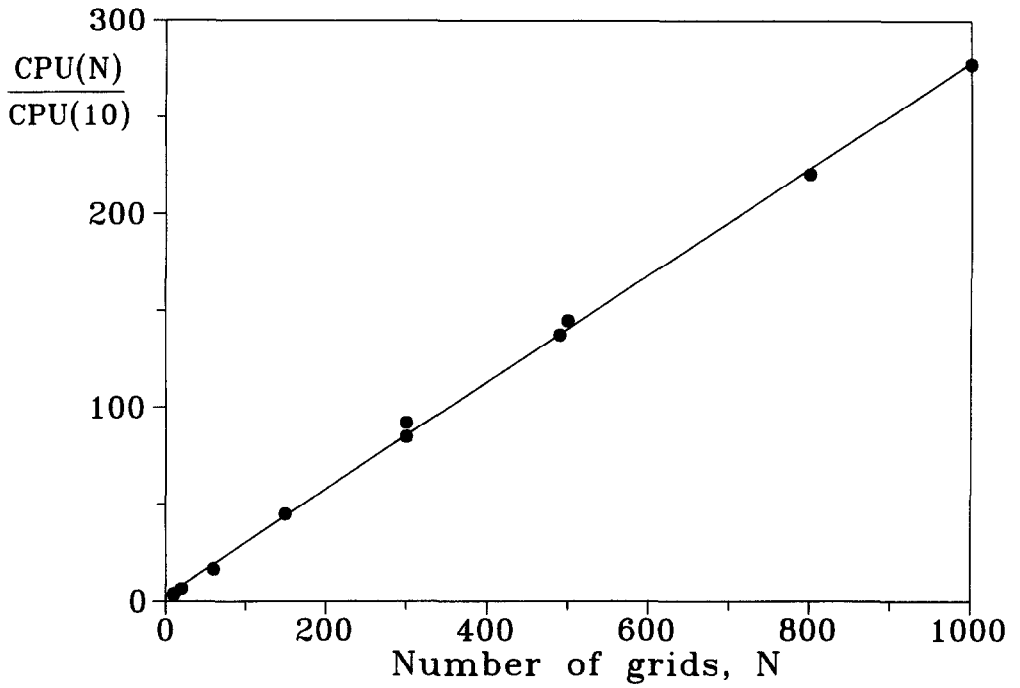

Fig. 4. Computational cost in terms of the total number of computational grids ($N = N_r \times N_z$).

These time constants can be used to determine quantitatively the relative importance of the heat exchange and heat conduction mechanisms. When t_h is small compared to t_λ, the system is mainly controlled by the heat conduction. On the other hand, the heat exchange is the main rate-limiting process when t_h is well larger than t_λ.

The global surface conductance can be easily derived from the above equation:

$$\frac{1}{h_{\text{eff}}} = \frac{1}{h_s} + \frac{2}{1-a^2}\left[\frac{1+a^2}{8} - \frac{a^2}{2}\left(\frac{a^2 \ln a}{1-a^2} + 1\right)\right]\frac{R_1}{\lambda_s}. \tag{30}$$

Similarly, when the heating is at the inner side, the zero-order moment of the volumetrically averaged temperature is given by:

$$\int_0^\infty \left(1 - \frac{\bar{T}_s - T_0}{T_1 - T_0}\right) dt = \frac{1-a^2}{2a}\frac{R_1 C_e}{h_s} + \left[\frac{1+a^2}{8} - \frac{1}{2}\left(\frac{\ln a}{1-a^2} + 1\right)\right]\frac{R_1^2 C_e}{\lambda_s} = t_h + t_\lambda \tag{31}$$

and the global surface conductance is equal to:

$$\frac{1}{h_{\text{eff}}} = \frac{1}{h_s} + \frac{2a}{1-a^2}\left[\frac{1+a^2}{8} - \frac{1}{2}\left(\frac{\ln a}{1-a^2} + 1\right)\right]\frac{R_1}{\lambda_s}. \tag{32}$$

6. RESULTS AND DISCUSSION

As the standard case for numerical investigations, we consider an adsorptive heat pump system using the zeolite NaX–ammonia pair. A previous study has demonstrated that as a result of high working pressures of ammonia, the uniform pressure assumption is satisfactory for usual bed permeabilities [19]. The adsorption equilibrium relation for this system is given by the Dubinin–Radushkevich equation [20]:

$$q = 221.2 \exp\left[-1.916 \times 10^{-7}\left(T \ln \frac{P_s}{P}\right)^2\right] (\text{kg m}^{-3}) \tag{33}$$

where q is based on the apparent volume of the adsorbent and the saturated vapor pressure of ammonia, P_s, is defined by:

$$P_s = 23.0272 - \frac{2748.39}{T} (\text{Pa}) \tag{34}$$

The external heating configuration will be chosen in the subsequent simulations. The values of the other physical and geometrical parameters are given in Table 1. When not specified, the cycle time will be set to be 240 s with equal times for the heating and the cooling, and the apparent thermal conductivity of the bed has a value of 5 W m^{-1} K^{-1}. In all the cases, sufficiently small values for the time step size will be used to ensure the numerical accuracy. This was verified by comparing numerical simulations obtained with well different time step sizes. The cyclically steady state was estimated to be attained when the relative difference of the pressure and temperatures obtained

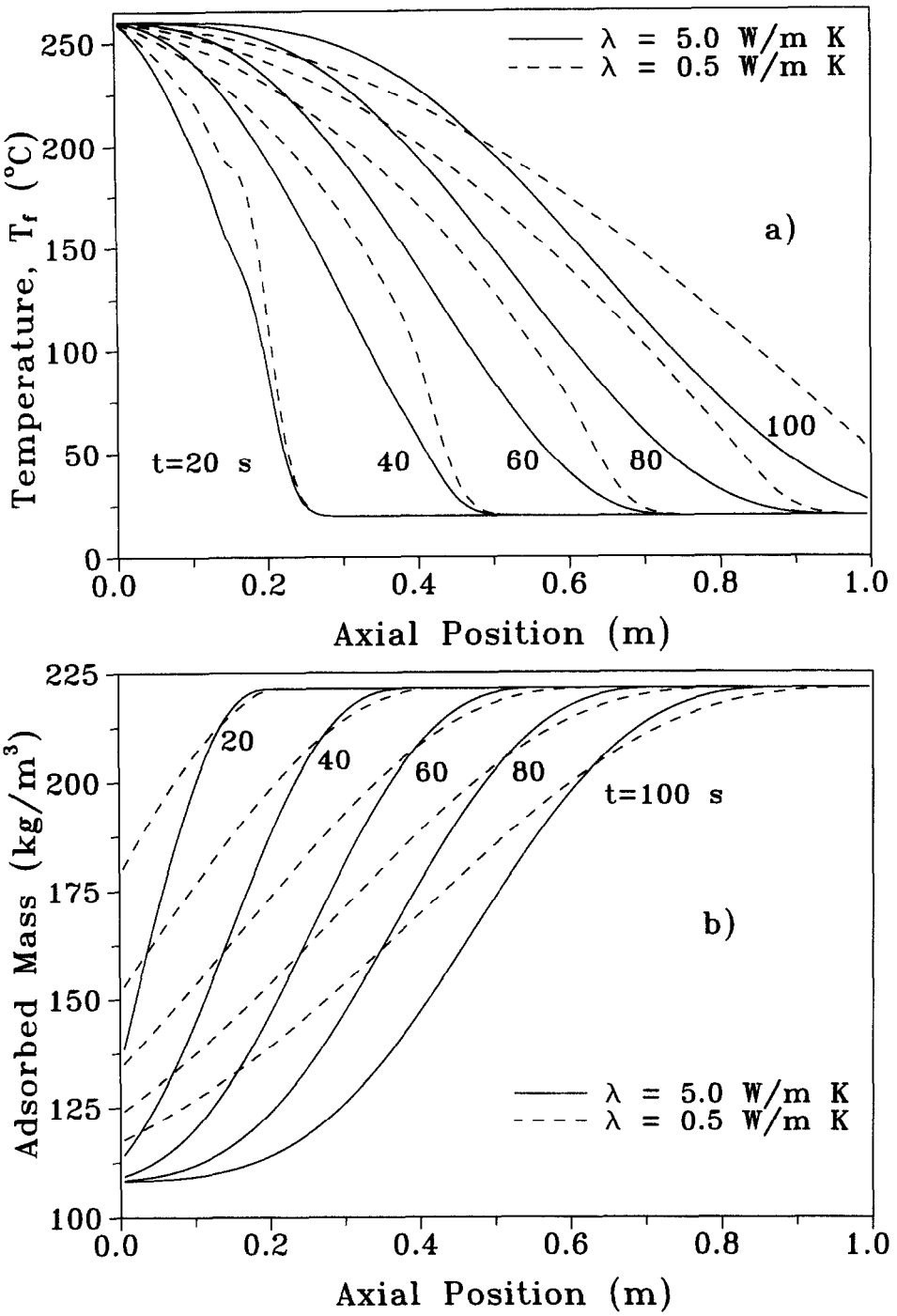

Fig. 5. Axial profiles of the fluid temperature T_f (a) and the adsorbed mass averaged over the bed section $\bar{q}$ (b) during the heating stage of the first cycle for two values of the apparent thermal conductivity: $\lambda_s = 0.5$ W m^{-1} K^{-1} (dashed lines) and $\lambda_s = 5$ W m^{-1} K^{-1} (solid lines). The cycle time is 240 s.

between two cycles becomes less than 10^{-4}. In this work, 10–50 cycles are generally needed, depending on the values of the model parameters used, especially on the cycle time. For the choice of numbers of computational grids to be used in the radial and axial directions, several simulations have been made using increasing numbers of grids. The results are shown in Fig. 3, wherein the cooling *COP*s obtained at the cyclically steady state are plotted. It can be seen that, for the present case, use of six grids in the radial direction and 100 grids in the axial direction is enough to ensure sufficient accuracies. The corresponding *COP* values differ only by less than 0.5% from the values obtained with significantly more grids. Therefore, these two values will be retained in the subsequent simulations. Note that many more grids are

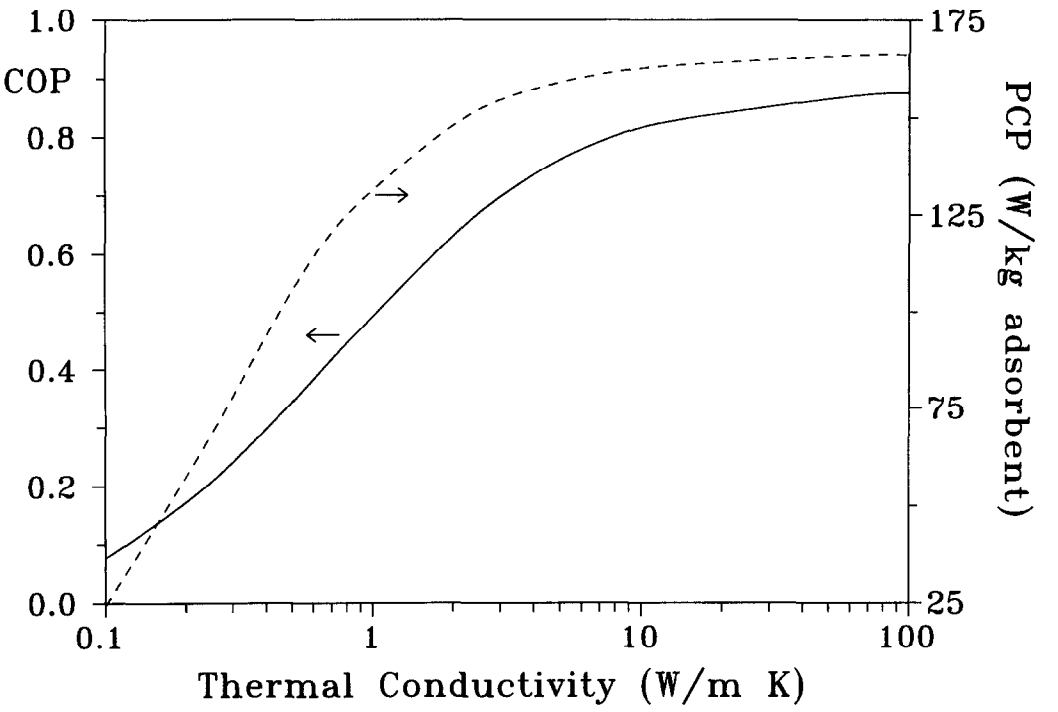

Fig. 6. Variations of the cooling *COP* and the mean power of cold production per unit of adsorbent mass, *PCP*, with the apparent thermal conductivity of the adsorbent bed.

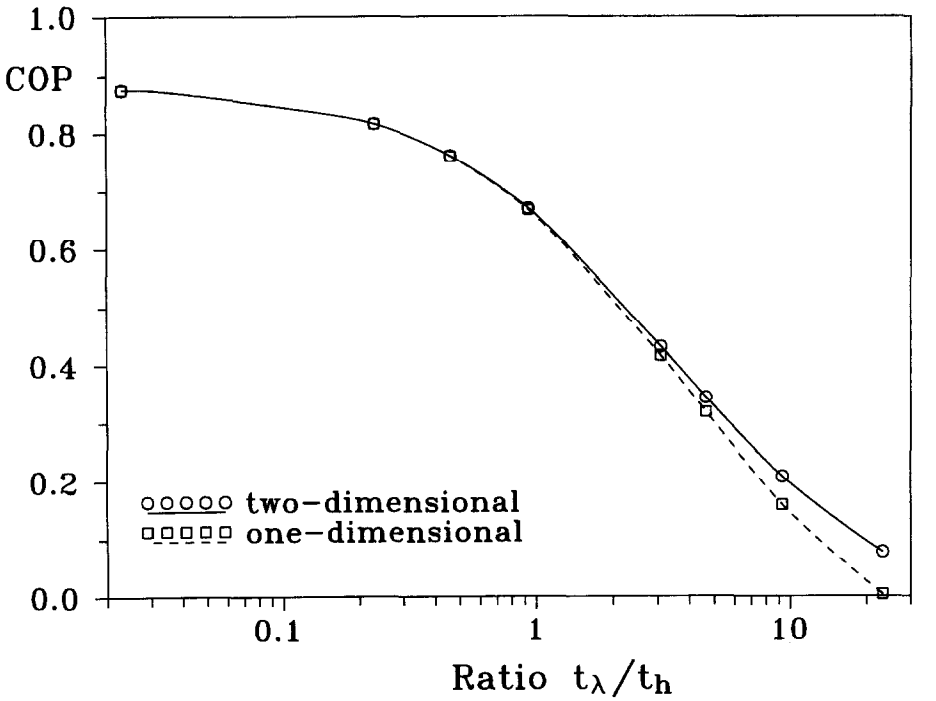

Fig. 7. Comparison of the *COP* values calculated by the two-dimensional model (solid line) and the one-dimensional model using the global unit surface conductance given in equation (30) (dashed line).

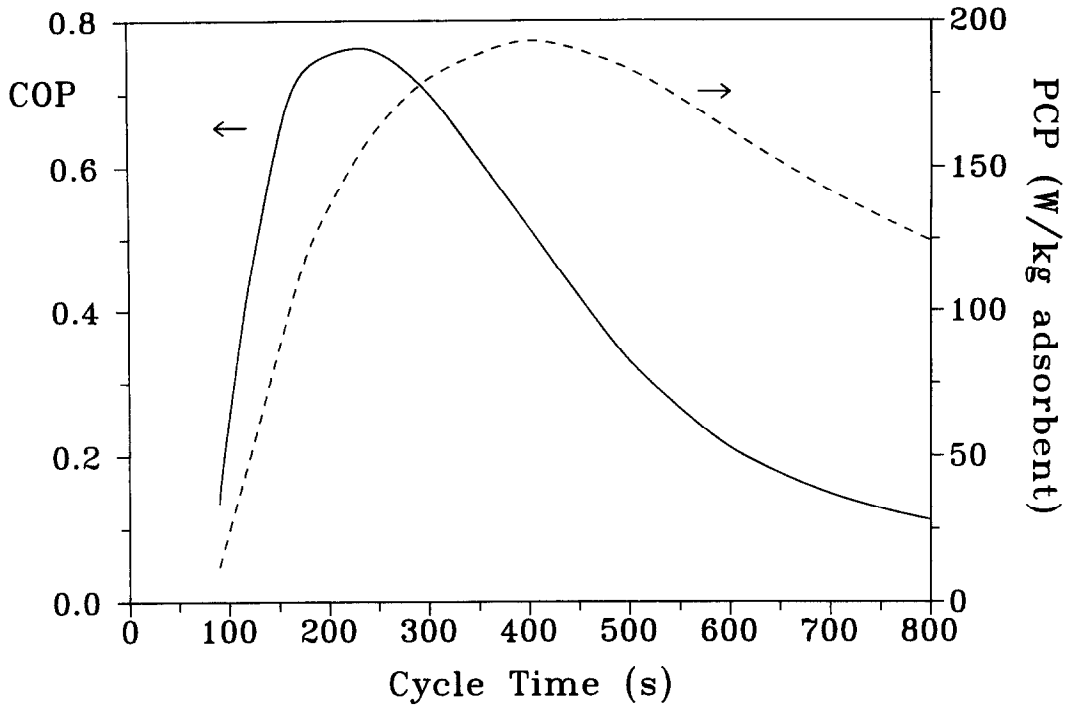

Fig. 8. Variations of the cooling *COP* and the *PCP* with the cycle time.

needed in the axial direction due to the large aspect ratio value used in this work ($L/R_1 = 100$). Numerical experiments have also shown that with the numerical method proposed by this work, the computation cost increases only linearly with the total number of grids (Fig. 4).

In Fig. 5, we present first axial profiles for the fluid temperature, T_f, and the adsorbed mass averaged over the whole section $[R_0, R_1]$, $\bar{q}$, at different times during the heating mode of the first cycle. Two values of the apparent thermal conductivity were used: $\lambda_s = 0.5$ (dashed lines) and $\lambda_s = 5$ W m^{-1} K^{-1} (solid lines). For a smaller thermal conductivity, the heat transfer resistances caused by heat conduction are larger and the temperature fronts of the fluid become more dispersed. Moreover, the adsorbent bed receives less heat energy, leading to a smaller quantity of adsorbate desorbed. The effect of the thermal conductivity on the process performance (*COP* and *PCP*) is shown in Fig. 6. As expected, both the *COP* and the *PCP* increase with the thermal conductivity. In particular, the *COP* drops from 0.87 to 0.21 when the apparent thermal conductivity is decreased from 100 to 0.25 W m^{-1} K^{-1}. Note that the apparent thermal conductivity of a traditional bed packed with granular particles is generally very small and is in the range of 0.1–0.2 W m^{-1} K^{-1} [21]. With such a bed, the resulting performance is clearly very poor. The high value of the thermal conductivity used in this work, 5 W m^{-1} K^{-1}, corresponds a value which can be obtained with a consolidated adsorbent [22].

In the previous section, we have given a definition of the global unit surface conductance accounting for both heat exchange and heat conduction processes. In order to check the validity of this definition, we have compared the numerical results obtained using the detailed model and the simplified one-dimensional model. In the latter case, the heat conduction is considered only through a global coefficient and only the simplified equation (23) is solved by using h_{eff} defined in equation (30) in the place of h_s. The comparison is presented in Fig. 7, wherein is plotted the *COP* vs the ratio of the time constants t_λ/t_h. It can be observed that the agreement between the two models is excellent when the ratio t_λ/t_h is inferior to 1. In this case, a detailed solution of the heat conduction equation is not necessary and the simplifying one-dimensional model gives satisfactory results provided that the global surface conductance defined in equation (30) and (32) is used.

Figure 8 presents the variations of the cooling *COP* and the mean power of cold production per unit of adsorbent mass, *PCP*, with the cycle time. It can be seen that both the *COP* and the *PCP* exhibit an optimum. The initial increase of the *PCP* with the cycle time is essentially due to the increase of the cycled adsorbate mass. However, at sufficiently long cycle times, the cycled adsorbate mass attains almost its maximum and a further increase of the cycle time gives only very small changes of the cycled mass, causing the *PCP* to decrease almost linearly with the cycle time. The maximum of the cooling *COP* is a result of the competition between the efficiency of adsorption/desorption and the efficiency of heat regeneration. In

a short cycle, the cycled mass of adsorbate is low and consequently the *COP* is small. On the other hand, when the cycle time is too long, the fluid temperature at the adsorber exit is increased or decreased too much, leading to a poor efficiency of the heat regeneration process. This effect explains the decrease of the *COP* with the cycle time after the maximum. From a practical point of view, the cycle should not be shorter than that corresponding to the maximum *COP*, as both the *COP* and the *PCP* would be very low at shorter cycle times. In this case, the optimal cycle time would be around the intersection of the *COP* and *PCP* curves (Fig. 8).

7. CONCLUSIONS

A numerical analysis of adsorptive heat pumps with thermal wave heat regeneration has been presented. The analysis has been based on a two-dimensional model which considered axial heat transfer in the fluid and radial heat conduction in the adsorbent bed. The gas pressure has been assumed to be uniform throughout the bed in the model development. This assumption is reasonable for heat pump systems using high-pressure adsorbates like ammonia. An efficient method of solution has been proposed and allows to solve the current two-dimensional problem in a one-dimensional way by neglecting the axial heat conduction inside the adsorbent bed. The numerical method has proven to have an optimal efficiency.

A new definition of the global unit surface conductance for the adsorbent bed has been derived using the moment analysis. This global coefficient can be used in a simplifying one-dimensional model in which solution of the radial heat conduction equation is avoided. The results agree well with those obtained by the detailed model when the ratio of the time constants for heat conduction and heat exchange, t_i/t_h, is small (<1). Furthermore, the two time constants derived in this work can be used directly to quantify the relative importance of the two heat transfer processes. This gives an easy way to determine which of the two processes is rate-limiting and needs to be improved.

This work has also confirmed that the performance of an adsorptive heat pump system using a traditional packed-bed would be too low, even with a heat regeneration, and therefore a significant enhancement of heat transfer properties inside the adsorber is necessary.

REFERENCES

1. N. Douss, F. Meunier and L. M. Sun, Predictive model and experimental results for a two-adsorber solid adsorption heat pump, *I&EC Res.* **27,** 310–316 (1988).
2. R. E. Critoph, Forced convection enhancement of adsorption cycles, *Heat Recovery Systems CHP* **14,** 343–350 (1994).
3. A. Boubakri, M. Arsalane, B. Yous, L. Ali-Moussa, M. Pons, F. Meunier and J. J. Guilleminot, Experimental study of adsorptive solar powered ice makers in Agadir (Morocco). Part 1: performance in actual site, *Renewable Energy* **2,** 7–13 (1992).
4. L. A. Luo and M. Feidt, Thermodynamics of adsorption cycles: a theoretical study, *Heat Transfer Engng* **13,** 1–13 (1992).
5. F. Meunier, Solid adsorption: an alternative to CFCs, *Heat Recovery Systems CHP* **13,** 289–295 (1993).
6. D. I. Tchernev, Heat pump energized by low-grade heat source, *U.S. Patent*, 4 637 218 (1987).
7. S. V. Shelton, Solid adsorbent heat pump system. *U.S. Patent*, 4 610 148 (1986).
8. S. V. Shelton, W. J. Wepfer and D. J. Miles, External fluid heating of a porous bed, in *Heat Transfer in Porous Media and Particulate Flows*, HTD-Vol. 46, pp. 77–83. ASME, New York (1985).
9. S. V. Shelton, W. J. Wepfer and D. J. Miles, Square wave analysis of the solid–vapor adsorption heat pump, *Heat Recovery Systems CHP* **9,** 233–247 (1989).
10. S. V. Shelton and D. J. Miles, Coupled heat transfer and thermodynamic adsorption heat pump analysis, in *Heat Pump Design, Analysis and Applications*, Vol. 26, pp. 33–38. ASME-AES, New York (1990).
11. R. J. Nunge and W. N. Gill, Mechanisms affecting dispersion and miscible displacement, in *Flow through Porous Media*. American Chemical Society Publications, Washington, DC (1970).
12. L. M. Sun and M. D. LeVan, Numerical solution of diffusion equations by the finite difference method: efficiency improvement by iso-volumetric spatial discretization, *Chem. Engng Sci.* **50,** 163–166 (1995).
13. D. U. von Rosenberg, *Methods for the Numerical Solution of Partial Differential Equations*. Gerald L. Farrar & Assoc., Tulsa, AZ (1977).
14. B. P. Leonard, A stable and accurate convective modelling procedure based on quadratic upstream interpolation. *Comput. Meth. Appl. Mech. Engng* **19,** 59–98 (1979).
15. L. M. Sun and F. Meunier, An improved finite difference method for fixed-bed multicomponent sorption. *AIChE. J.* **37,** 244–254 (1991).
16. W. H. Press, B. P. Flannery, S. A. Teukolsky and W. T. Vetterling, *Numerical Recipes*. Cambridge University Press, Cambridge (1986).
17. D. M. Ruthven, *Principles of Adsorption and Adsorption Processes*. Wiley Interscience, New York (1984).
18. L. M. Sun, F. Meunier, Ph. Grenier and D. M. Ruthven, Frequency response of nonisothermal adsorption in biporous pellets, *Chem. Engng Sci.* **49,** 373–381 (1994).
19. L. M. Sun, N. Ben Amar and F. Meunier, Numerical study on coupled heat and mass transfers in an adsorber with external fluid heating, *Heat Recovery Systems CHP* **15,** 19–29 (1995).
20. R. E. Critoph and L. Turner, Performance of ammonia-activated carbon and ammonia-zeolite heat pump adsorption cycles. *Proc. Pompes à chaleur chimiques de hautes performances*. Lavoisier, Perpignan (1988).
21. L. Onyebueke and M. Feidt, Apparent thermal conductivity of granular active charcoal in presence of inert gas of reactive vapors, *J. High Temp. High Press.* **24,** 409–414 (1992).
22. J. J. Guilleminot, A. Choisier, J. B. Chalfen, S. Nicolas and J. L. Reymoney, Heat transfer intensification in fixed bed adsorbers, *Heat Recovery Systems CHP* **13,** 297–300 (1993).

APPENDIX A

The solution of equation (26) in the Laplace domain is:

$$\tilde{\theta}(s) = c_1 I_0(\alpha r) + c_2 K_0(\alpha r) \left(\alpha = \sqrt{\frac{s}{\lambda_s / C_e}} \right)$$

where $\theta = (T - T_0)/(T_1 - T_0)$ is the normalized temperature, I_0 and K_0 are zero-order modified Bessel functions of first and second kind, c_1 and c_2 are two constants to be determined from the boundary conditions. For the outer heating:

$$c_1 = \frac{h_s K_1(\alpha R_0)}{K_1(\alpha R_0)[h_s I_0(\alpha R_1) + \lambda_s \alpha I_1(\alpha R_1)] + I_1(\alpha R_0)[h_s K_0(\alpha R_1) - \lambda_s \alpha K_1(\alpha R_1)]}$$

$$c_2 = \frac{h_s I_1(\alpha R_0)}{K_1(\alpha R_0)[h_s I_0(\alpha R_1) + \lambda_s \alpha I_1(\alpha R_1)] + I_1(\alpha R_0)[h_s K_0(\alpha R_1) - \lambda_s \alpha K_1(\alpha R_1)]}.$$

For the inner heating:

$$c_1 = \frac{h_s K_1(\alpha R_1)}{K_1(\alpha R_1)[h_s I_0(\alpha R_0) - \lambda_s \alpha I_1(\alpha R_0)] + I_1(\alpha R_1)[h_s K_0(\alpha R_0) + \lambda_s \alpha K_1(\alpha R_0)]}$$

$$c_2 = \frac{h_s I_1(\alpha R_1)}{K_1(\alpha R_1)[h_s I_0(\alpha R_0) - \lambda_s \alpha I_1(\alpha R_0)] + I_1(\alpha R_1)[h_s K_0(\alpha R_0) + \lambda_s \alpha K_1(\alpha R_0)]}.$$

The volumetrically-averaged normalized temperature is given by:

$$\tilde{\theta} = \frac{2}{R_1^2 - R_0^2}\int_{R_0}^{R_1} \theta r \, dr$$

$$= \frac{2}{\alpha(R_1^2 - R_0^2)}\{c_1[R_1 I_1(\alpha R_1) - R_0 I_1(\alpha R_0)] + c_2[R_0 K_1(\alpha R_0) - R_1 K_1(\alpha R_1)]\}.$$

Then, the zero-order moments can be determined by using van der Laan's theorem:

$$\int_0^\infty (1 - \bar{\theta})\, dt = \lim_{s \to 0}\left(\frac{1}{s} - \tilde{\bar{\theta}}\right).$$

The final solutions of the zero-order moments are given in equations (29) and (31).

APPENDIX B

Consider the case where the heat transfer fluid is at the outside of the adsorbent bed. The finite difference analogs of the heat conduction equation (13) together with its boundary conditions (16–17) can be written as:

$$b_1 T_{s1,j}^{n+1} + c_1 T_{s2,j}^{n+1} = d_1$$

$$a_i T_{si-1,j}^{n+1} + b_i T_{si,j}^{n+1} + c_i T_{si+1,j}^{n+1} = d_i \quad (i = 2, 3, \ldots, N_r - 1)$$

$$a_{N_r} T_{sN_r-1,j}^{n+1} + b_{N_r} T_{sN_r,j}^{n+1} = d_{N_r} - \Gamma T_{mj}^{n+1}$$

where a, b, c, d and Γ are coefficients obtained after the finite difference approximations.

Perform first the forward calculation:

$$\beta_1 = b_1; \quad W_1 = \frac{d_1}{\beta_1}$$

$$\beta_i = b_i - \frac{a_i c_{i-1}}{\beta_i}; \quad W_i = \frac{d_i - a_i W_{i-1}}{\beta_i} \quad (i = 2, \ldots, N_r).$$

Then, the backward solution is made for the determination of the coefficients $F_{i,j}$ and $G_{i,j}$:

$$F_{N_r,j} = W_{N_r}; \quad G_{N_r,j} = -\frac{\Gamma}{\beta_{N_r}}; \quad F_{i,j} = W_i - \frac{c_i}{\beta_i} F_{i+1,j};$$

$$G_{i,j} = -\frac{c_i}{\beta_i} G_{i,j} \quad (i = N_r - 1, N_r - 2, \ldots, 1).$$